

Supporting information

Near ultra-violet to mid-visible band gap tuning of mixed cation

$\text{Rb}_x\text{Cs}_{1-x}\text{PbX}_3$ (X=Cl or Br) perovskite nanoparticles

Daniel Amgar, Tal Binyamin, Vladimir Uvarov, Lioz Etgar*

The Institute of Chemistry, The Center for Nanoscience and Nanotechnology, The Casali Center for Applied Chemistry, The Hebrew University of Jerusalem, Jerusalem, Israel

*E-mail: lioz.etgar@mail.huji.ac.il

ions	effective ionic radii (Å)	x values	r_A (Å)	t (X=Cl)	t (X=Br)	t (X=I)
Cs ⁺	1.74	0.0	1.74	0.837	0.830	0.822
Rb ⁺	1.61	0.2	1.71	0.830	0.825	0.816
Pb ⁺	1.19	0.4	1.67	0.824	0.819	0.811
Cl ⁻	1.81	0.6	1.66	0.818	0.813	0.806
Br ⁻	1.96	0.8	1.64	0.812	0.807	0.800
I ⁻	2.20	1.0	1.61	0.806	0.801	0.795

Table S1. The parameters used to calculate the effective tolerance factors (t) of $\text{Rb}_x\text{Cs}_{1-x}\text{PbX}_3$ (x=Rb content, X=Cl, Br, I), according to the tolerance factor formula. r_A is the calculated effective ionic radius of “A” cation in AMX_3 perovskite structure considering the different ratios between Cs⁺ and Rb⁺ by x being the Rb⁺ content.

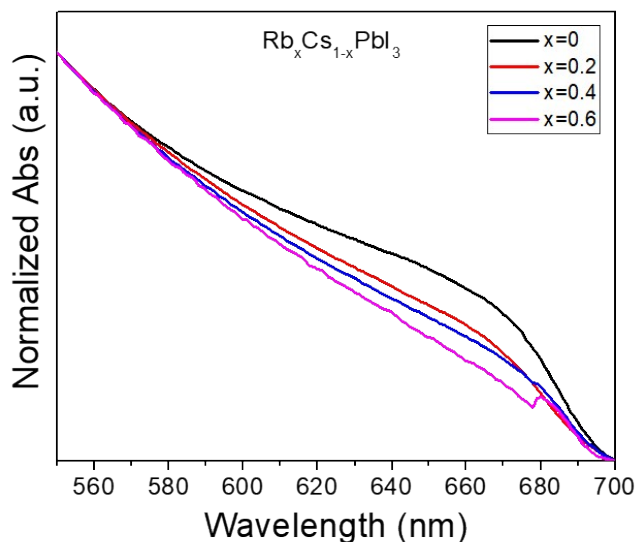


Figure S1. Absorbance spectrum of $\text{Rb}_x\text{Cs}_{1-x}\text{PbI}_3$ NPs.

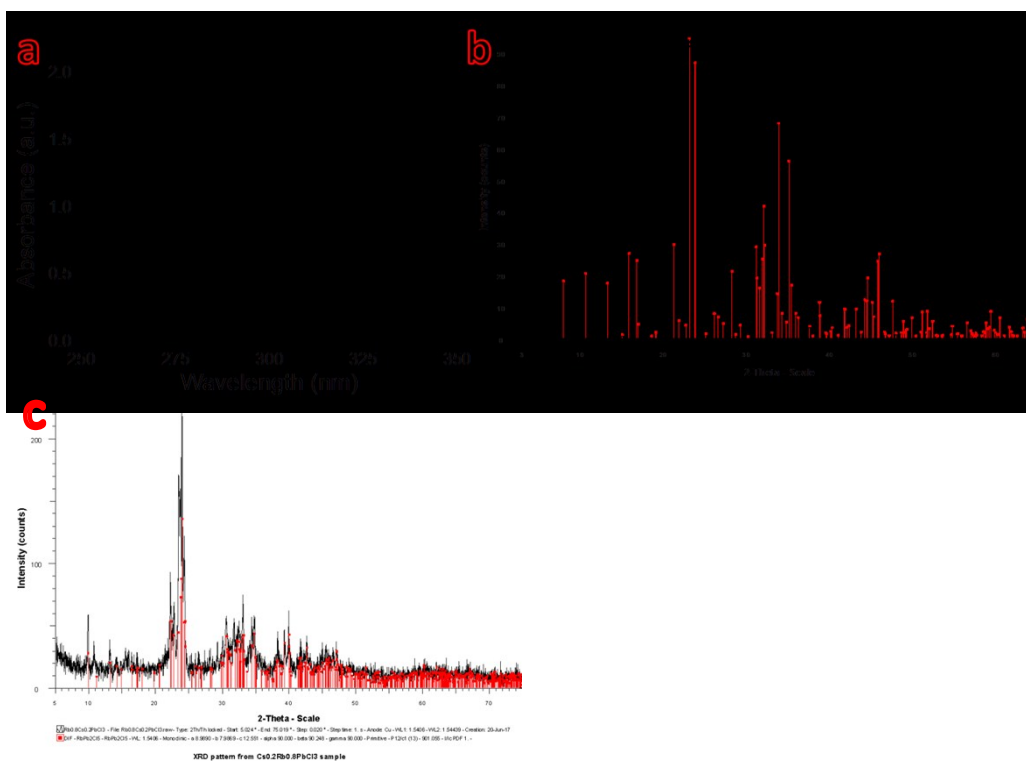


Figure S2. Absorbance spectrum (a) and XRD pattern of tetragonal $\text{Rb}_6\text{Pb}_5\text{Cl}_{16}$ NPs (b); XRD pattern of $\text{Cs}_{0.8}\text{Rb}_{0.2}\text{PbCl}_3$ sample (c)

	x=0	x=0.2	x=0.4	x=0.6	x=0.8	x=1
Cl	orthorhombic CsPbCl_3 rhombohedral Cs_4PbCl_6	orthorhombic CsPbCl_3	orthorhombic CsPbCl_3	orthorhombic CsPbCl_3 unidentified phase	monoclinic RbPb_2Cl_5 tetragonal $\text{Rb}_6\text{Pb}_5\text{Cl}_{16}$	tetragonal $\text{Rb}_6\text{Pb}_5\text{Cl}_{16}$
Br	orthorhombic CsPbBr_3	orthorhombic CsPbBr_3 orthorhombic Cs_4PbBr_6	orthorhombic CsPbBr_3	orthorhombic CsPbBr_3 tetragonal Rb_4PbBr_6 orthorhombic Cs_4PbBr_6	orthorhombic CsPbBr_3 tetragonal Rb_4PbBr_6	-----

Table S2. The detected phases from PXRD measurements for the $\text{Rb}_x\text{Cs}_{1-x}\text{PbX}_3$ (x=0, 0.2, 0.4, 0.6, 0.8; X=Cl, Br) NPs.

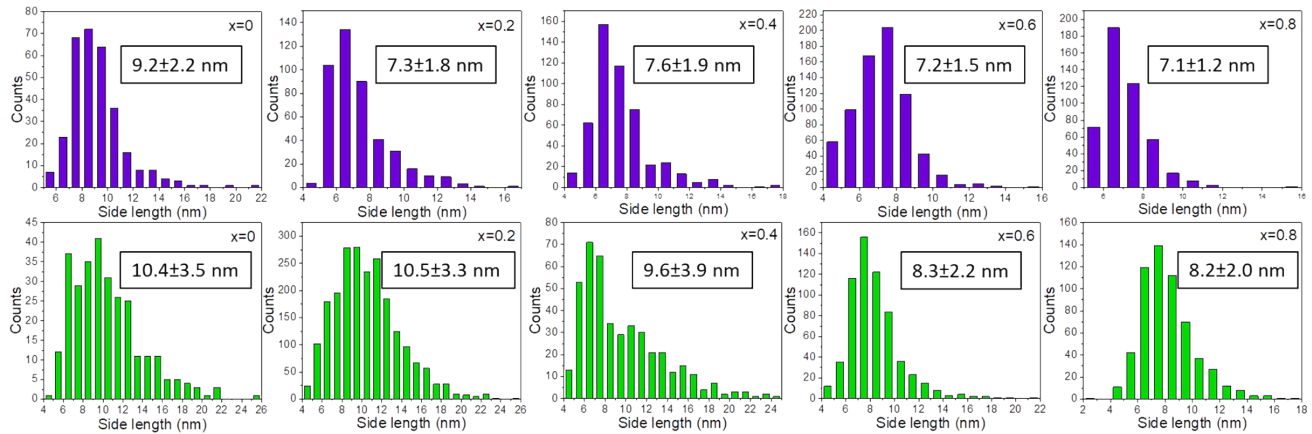


Figure S3. Size distribution histograms of $\text{Rb}_x\text{Cs}_{1-x}\text{PbX}_3$ ($x=0, 0.2, 0.4, 0.6, 0.8$; $X=\text{Cl}, \text{Br}$) NPs. The upper purple histograms are related to $\text{Rb}_x\text{Cs}_{1-x}\text{PbCl}_3$ and the lower are related to $\text{Rb}_x\text{Cs}_{1-x}\text{PbBr}_3$. The average side lengths of each product are written in the text boxes.

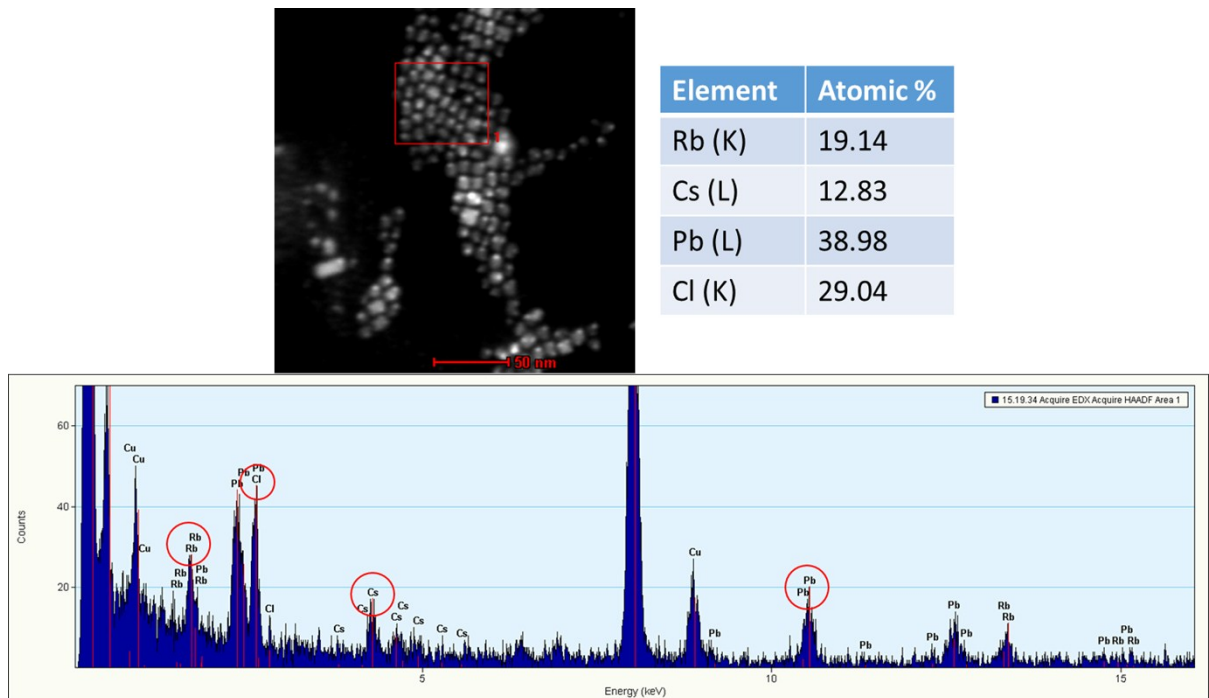


Figure S4. Energy dispersive x-ray spectroscopy (EDS) of $\text{Rb}_{0.8}\text{Cs}_{0.2}\text{PbCl}_3$ ($x=0.8$) NPs; EDS spectrum of the scanned area in the scanning transmission electron microscopy (STEM) image, and quantification of the detected elements: Rb, Cs, Pb, and Cl. The other peaks in the EDS spectrum are related to Cu and C, which are assigned to the carbon grid that is covered with amorphous carbon.

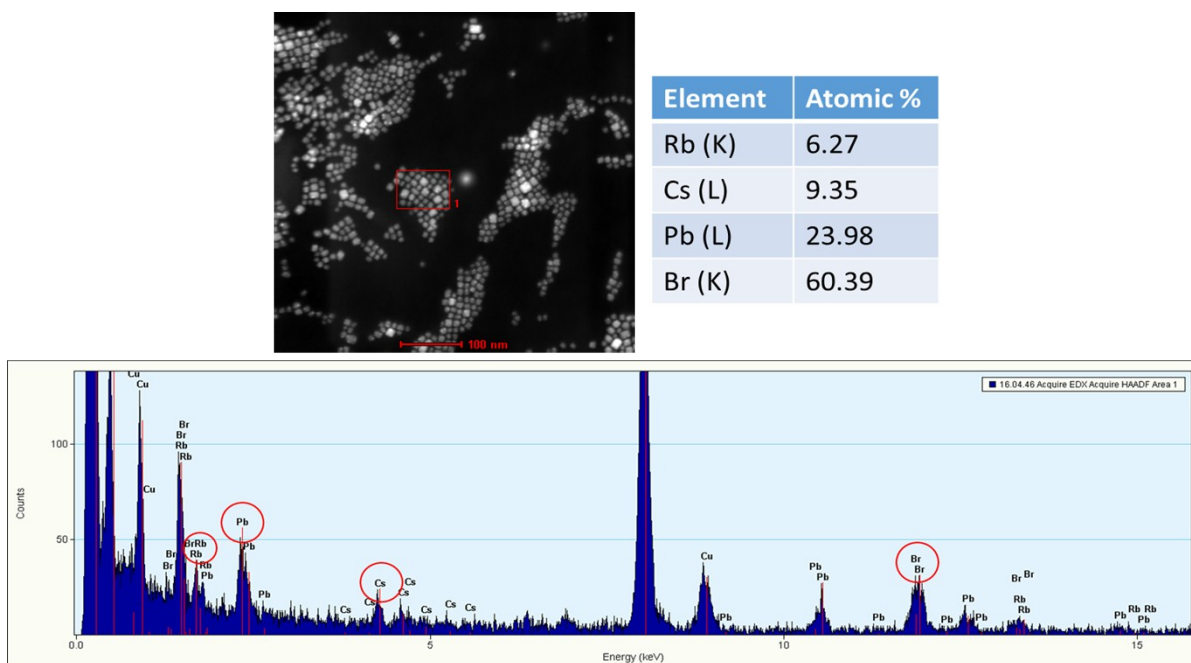


Figure S5. Energy dispersive x-ray spectroscopy (EDS) of $\text{Rb}_{0.8}\text{Cs}_{0.2}\text{PbBr}_3$ ($x=0.8$) NPs; EDS spectrum of the scanned area in the scanning transmission electron microscopy (STEM) image, and quantification of the detected elements: Rb, Cs, Pb, and Br. The other peaks in the EDS spectrum are related to Cu and C, which are assigned to the carbon grid that is covered with amorphous carbon.

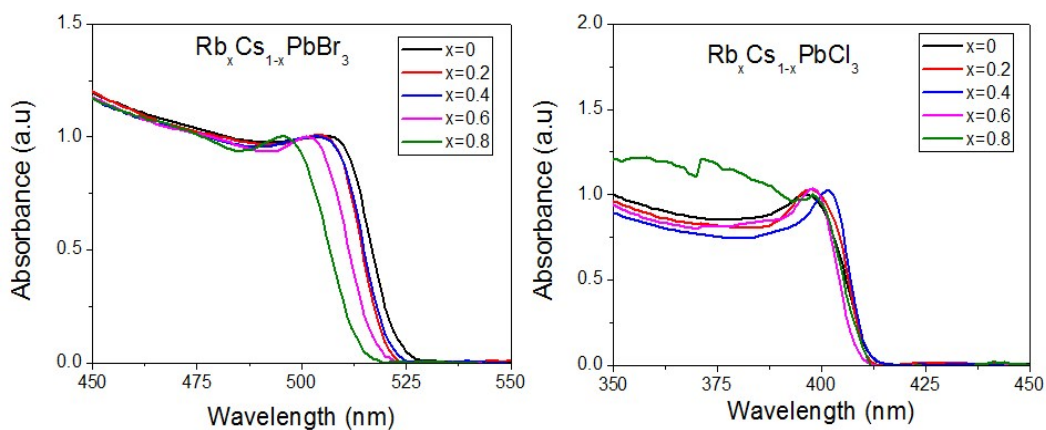


Figure S6. Absorption after a week from the day of synthesis.

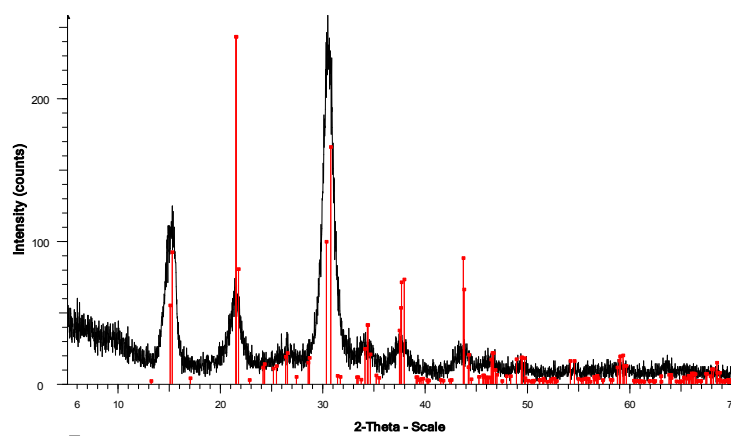


Figure S7: XRD for the control experiment with the formula $\text{Cs}_{0.2}\text{PbBr}_3$ in the orthorhombic phase.